

pubs.acs.org/journal/ascecg Research Article

# Toward Carbon-Negative and Emission-Curbing Roads to Drive **Environmental Health**

Hamid Ghasemi, Hessam Yazdani, Amirul Rajib, and Elham H. Fini\*



Cite This: ACS Sustainable Chem. Eng. 2022, 10, 1857-1862

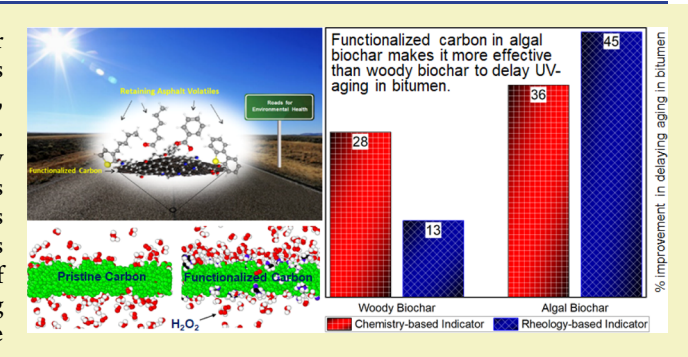


ACCESS I

Metrics & More

Article Recommendations

ABSTRACT: Roadway infrastructures are exposed to solar ultraviolet (UV) radiation during their service life. UV rays generate free radicals that diffuse deep into bitumen layers, accelerating the aging and degradation of bituminous composites. Here, we hypothesize that carbonaceous particles grafted by bioderived molecules such as amines and amides can serve as scavengers of free radicals, delaying aging in bituminous composites. To test this hypothesis, we use laboratory experiments and molecular dynamics simulations to compare the efficacy of biochars made from woody biomass and algal biomass in delaying the aging of bituminous composites. We further examine the underlying molecular mechanisms that delay aging by computing



the extent of diffusion of free radicals through an amorphous graphite film in the pristine form and in amine- and amidefunctionalized forms. The laboratory results indicate that algal biochar is considerably more effective than woody biochar in delaying aging. The simulation results corroborate laboratory findings showing that even at low concentrations, surface functionals such as amines and amides considerably enhance the efficacy of pristine carbon in shielding the underlying layers against the diffusion of free radicals such as hydrogen peroxide (H<sub>2</sub>O<sub>2</sub>). At high concentrations (e.g., 10 wt %), amines were found to be more effective than amides in reducing the diffusion rate of  $H_2O_2$ . This indicates that the scavenging efficacy of carbonaceous particles can be optimized by proper biografting. The algae that were used to make functionalized carbonaceous particles in this study are a means to capture CO<sub>2</sub> from air. Therefore, our findings contribute to extending the sustainability of highway infrastructures while moving toward carbon-negative and emission-curbing roads to promote environmental health.

KEYWORDS: sustainability, biogenic carbon, aging, free radicals, surface functional

## **■** INTRODUCTION

Ultraviolet (UV) exposure generates reactive oxygen species (ROS) such as hydrogen peroxide  $(H_2O_2)$  that later decompose into free radicals. These free radicals react rapidly with oxygen to form a variety of new products including polar oxygenous (O-containing) compounds such as ketones, sulfoxides, and carboxylic acids. If diffused into the bituminous structure of pavements, free radicals and their derivative compounds can accelerate age hardening in pavements through mechanisms such as chain scission, aromatization, carbonation, and loss of volatiles. Accelerated age hardening decreases the long-term performance of pavements and reduces the sustainability of the built environment.<sup>1,2</sup>

Microscopic characterization and nanoindentation of UVirradiated, 600 nm thick bitumen films have shown that the films became excessively hard and brittle after 20 h of UV exposure and experienced substantial mass loss after 50 h of UV exposure.<sup>3</sup> UV exposure affects the surface and bulk properties of bituminous composites differently. A comparison of the morphology and chemical composition of the surface

and bulk of nonaged and UV-aged thin bitumen films has shown that sulfur hydroxyls, phenyls, and CH<sub>3</sub> groups present in the bulk were absent or depleted from the surface.2

The combined effect of heat and solar radiation has particularly proven harmful to pavements by increasing the emission of aromatics that in turn accelerates the loss of bitumen compounds. Khare et al.4 showed a 2-fold increase in gaseous emissions and potential secondary organic aerosol (SOA) production as a result of summertime-resembling temperatures rising from 40 to 60 °C. Each additional 20 °C increment in the temperature up to 140 °C was associated with on average 70% more gaseous emissions and SOA production. This study reported a nearly 300% increase in total emissions

October 29, 2021 Received: January 10, 2022 Revised: Published: January 24, 2022





from road asphalt between two samples collected back-to-back without and with artificial sunlight; sulfur-containing compounds showed the greatest increase (700%), followed by oxygenous compounds (400%) and hydrocarbons (300%).

Various minerals and nanoparticles have shown promise in delaying the aging of bitumen: polyphosphoric acid, nanosilica, nanoclay, 5-7 carbon black, and carbon nanoplatelets. 8,9 For instance, the addition of 5 wt % layered double hydroxides (LDHs) as a UV-resistant material to bitumen enhanced the UV-aging resistance and low-temperature properties of the bitumen. However, another study indicated that organic intercalated LDHs were more effective in modifying bitumen than LDHs. 11 Triethoxyvinylsilane surface-organic-modified LDHs (TEVS-LDHs) also performed better than LDHs in terms of the UV-aging resistance of bitumen. 12 It was found that after UV aging, bitumen became harder and more brittle, but the application of TEVS-LDHs alleviated the deterioration of the bitumen. 12 Cao et al. 13 tested the UV-aging resistance of bitumen samples containing LDHs of different particle sizes (75, 115, 180, and 300 nm); the samples modified with 180 nm LDHs exhibited the most-improved anti-UV-aging proper-

Algae and microalgae have proven promising in promoting sustainability. Besides having simple nutritional requirements, these phototrophic microorganisms offer high tolerance to elevated concentrations of CO<sub>2</sub> and flue gas, high growth rates, low requirements for light intensity, genetic tractability, and significant photosynthetic capacity. Algae and microalgae can serve as highly effective and efficient natural sinks for CO<sub>2</sub> sequestration. They also produce biomass rich in value-added products such as nutritional supplements, antioxidants, fertilizers, pharmaceuticals, and polyunsaturated fatty acids. In addition, microalgae offer a vast potential to produce biofuels such as biodiesel, bioethanol, biohydrogen, and biogas, offering a solution to both energy and environmental problems. <sup>16</sup>

Algal biomass also has the potential to turn the built environment into a durable, massive carbon sink and an inhibitor of gaseous emissions. Because algal biomass is rich in protein and nucleic acids, it yields biochar that is abundant with oxygenous groups (e.g., phenols, carboxyl, carbonyl, and ketene) and nitrogenous groups (e.g., amide, amine, pyrrole, and pyridine).<sup>17</sup> Some of these nitrogenous groups react with carboxyl groups such as -C=O via the Maillard reaction, forming more bonds with the biochar structure and resulting in improved adsorption characteristics. <sup>18,19</sup> These functional groups often have a stronger nonbonded interaction with intrusive precursors to free radicals such as H2O2 suggesting that they can slow the intrusion of such compounds via chemisorption<sup>20-22</sup> and physisorption<sup>23</sup> and offer enormous potential for adsorption of ROS and flue gas. If dispersed in bituminous composites such as asphalt pavements and shingles, algal biochar is expected to use these functional groups to retain compounds that would otherwise be emitted into the air, potentially serving as ozone precursors and negatively impacting air quality and human health. Algae and other biomass can also be used to produce rejuvenators to restore the thermomechanical properties of aged bitumen. 24-26

Here, we tested the hypothesis that surface functionals in algal biochar delay the diffusion of free radicals into bituminous composites. To do so, we compared the efficacy of biochars made from woody biomass and algal biomass in delaying the aging of bituminous composites. The delay in

aging was measured based on changes in the chemical and rheological properties of modified bitumen samples exposed to UV aging. We also used molecular dynamics simulations to gain an insight into the protection mechanism of amide and amine functional groups and to compare their efficacy in protecting a graphite film against the attack of  $\rm H_2O_2$  as a representative of free-radical precursors.

#### MATERIALS AND METHODS

Materials. The unaged neat binder (NB) was a PG 64-10-graded bitumen (Table 1). Algal biochar, hereafter also referred to as

Table 1. Properties of the PG 64-10 Binder

	test at temperature	result
original binder	flash point	302 °C
	rotational viscosity at 135 °C	0.402 Pa s
	dynamic shear rheometer, $G^*/\sin\delta$ at 64 °C	1.173 kPa
aged binder (aged at 100 °C)	dynamic shear rheometer, $G^*/\sin\delta$ at 31 °C	1182 kPa
	stiffness at 0 °C	28 MPa
	m-value at 0 °C	0.468

inherently functionalized carbon (IFC), was produced by the hydrothermal liquefaction (HTL) of algal biomass. THTL was performed at 330 °C in a 250-mL stainless-steel benchtop batch reactor (Parr Instrument Company, Moline, IL) equipped with a magnetic stirrer, a 4843 controller, and a jacketed heater. The working volume of the system was set to a maximum of 125 mL. IFC was produced at 20% solid loading (25 g dry weight) in all the HTL experiments. Conventional biochar, hereafter also referred to as pristine carbon (PC), was produced from woody biomass as detailed elsewhere. Biochar-filled bitumen samples were prepared by adding 5 wt % IFC or PC to NB and blending the mix with a shear mixer at 135 °C for 5 min. The blended samples were labeled as PC-modified binder (PCB) and IFC-modified binder (FCB).

**UV Aging Method.** Aged samples were prepared following a method described elsewhere. First, 0.65 mm thick films were prepared by evenly spreading 10 g of the unaged samples (NB, PCB, or FCB) on a steel pan that is 140 mm in diameter. The pan was then placed in a QUV accelerated weathering tester (Q-Lab Corporation, Westlake, OH) 100 mm from the lamp. The lamp delivered a UV radiation intensity of 0.71 W/m<sup>2</sup> at 313 nm. UV exposure was sustained for 200 h at 65 °C.

Dynamic Shear Rheometer. The elastic and viscous properties of each sample were measured using an Anton Paar rheometer MCR 302 following ASTM D7175-05. 30 The tests were carried out using an 8 mm, parallel-plate spindle at a 0.1% strain rate and frequencies ranging from 0.1 to 100 rad/s at 10 °C. The measured stress and strain data were used to calculate the shear modulus  $(G^*)$  and phase angle  $(\delta)$  based on eq 1. From the data, the modulus and frequency at which the phase angle was 45° were determined as crossover values. At the crossover point, the elastic modulus  $(G^{"})$  and the viscous modulus (G'') are equal. Considering that progressive aging leads to significant changes in polydispersity as asphaltene molecules form nanoaggregates, <sup>21,31</sup> crossover values are deemed appropriate to track the evolution of bitumen not only during aging but also during rejuvenation.<sup>32</sup> Provided that the crossover frequency and the corresponding crossover moduli are measured at the same temperature for all bitumen specimens in comparison, the crossover values can properly detect and compare the extent of aging and, in this study, the extent of the delay in aging

$$G^* = \frac{\tau_{\text{max}}}{\tau_{\text{max}}} \tag{1}$$

where  $\gamma_{\text{max}} = \theta r/h$ ,  $\tau_{\text{max}} = 2T/\pi r^3$ ,  $\gamma_{\text{max}}$  is the maximum strain,  $\tau_{\text{max}}$  is the maximum stress, T is the maximum torque applied, r is the radius

of the sample,  $\theta$  is the deflection (rotational) angle, and h is the height of the sample.

**Rheological Aging Index.** The rheological aging index was calculated based on the change in the crossover modulus, which has proven to be highly sensitive to aging.<sup>33,34</sup> The rheological aging index for each scenario was calculated as

Rheological aging index

$$= \frac{\text{unaged crossover modulus} - \text{aged crossover modulus}}{\text{unaged crossover modulus}} \times 100 \tag{2}$$

**FTIR Spectroscopy.** A Bruker Fourier transform infrared (FTIR) spectrometer (Bruker Corporation) was used to characterize the functional groups of unaged and UV-aged samples. Before starting the test, the FTIR diamond crystal surface was cleaned with isopropanol. Each FTIR spectrum was collected from 400 to 4000 cm<sup>-1</sup> wavenumbers with a resolution of 4 cm<sup>-1</sup> with 32 scans. The sample spectra were normalized against the background spectrum. OMNIC software v. 9.2.86 was used to analyze the peaks and calculate the area under each peak.

**Chemical Aging Index.** FTIR spectroscopy was used to track the extent of change in the chemical structure of bitumen during aging.<sup>3</sup> To quantify the change, eqs 3 and 4 were used to calculate the carboxyl functional groups and sulfoxide functional groups of all samples. The chemical aging index was calculated using eqs 5 and 6.

Carbonyl index = 
$$\frac{\text{area under curve from 1680 to 1800 cm}^{-1}}{\text{area under curve from 600 to 4000 cm}^{-1}} \times 100$$

$$\times 100$$
Sulfoxide index = 
$$\frac{\text{area under curve from 960 to 1050 cm}^{-1}}{\text{area under curve from 960 to 1050 cm}^{-1}}$$

Sulfoxide index = 
$$\frac{\text{area unider curve from } 600 \text{ to } 1030 \text{ cm}^{-1}}{\text{area under curve from } 600 \text{ to } 4000 \text{ cm}^{-1}} \times 100$$

Chemical index = carbonyl index + sulfoxide index 
$$(5)$$

Chemical aging index

$$= \frac{\text{aged chemical index} - \text{unaged chemical index}}{\text{unaged chemical index}} \times 100$$
(6)

Molecular Dynamics Simulations. Molecular dynamics (MD) simulations were carried out to study the efficacy of amide and amine functional groups in protecting biochar against the diffusion of hydrogen peroxide (H2O2). The FTIR spectra of the algal biochar produced and tested in this study displayed peaks in the range 1600-1670 cm<sup>-1</sup>, indicating the presence of a combination of aromatic ring stretching, alkene C=C stretching, C=O, and amine/amide N-H deformation modes.<sup>27</sup> Studies on the formation and evolution of nitrogenous species during the combustion, 35 HTL, 36 and pyrolysis 37 of biomass and algae corroborate the existence of these species. Their relative abundance, however, depends on the biomass composition and the interactions among its constituents and their derivatives as well as external nitrogen sources.<sup>38</sup> In light of this variability, nonadecanamide  $(C_{19}H_{39}NO)$  and ethylenediamine  $(C_{2}H_{4}(NH_{2})_{2})$ were used to represent the amide and amine functional groups in algal biochar, respectively. The selection of ethylenediamine was also based on the expectation that the results would benefit research on its application as a functional for CO<sub>2</sub> capture.<sup>39,40</sup> Biochar was modeled as an amorphous graphite film. Five steps were taken to construct the film:  $^{41}$  (1) a stack of five graphene sheets of dimensions of 5 nm  $\times$  5 nm with an interlayer spacing of 0.335 nm was placed in the simulation box. (2) The temperature was increased at a constant volume from 300 to 6000 K using the Nose-Hoover (NH) thermostat over 50 ps. (3) The temperature was maintained at 6000 K for another 50 ps to allow for the formation of an amorphous structure. (4) The structure was quenched by lowering the temperature back to 300 K over 0.5 ps, preventing the sheets from

restoring their initial configuration. (5) The temperature was kept at 300 K at constant zero pressure using the NH thermostat for 20 ps to achieve the final structure. A time step of 1 fs was used, and the reactive force-field (ReaxFF) potential<sup>42</sup> was used to represent interatomic interactions.

The diffusion of  $H_2O_2$  into the constructed biochar film in both pristine and functionalized forms was simulated, and the number of  $H_2O_2$  molecules having passed the film at a given time was used to compare different cases. The simulation of  $H_2O_2$  diffusion through pristine biochar involved the following three steps: (1) a reservoir of 300  $H_2O_2$  molecules was positioned at a minimum distance of 4 Å above the biochar film. (2) The temperature was set at 300 K using the Langevin algorithm. (3) The biochar film and  $H_2O_2$  molecules were allowed to interact with one another for 20 ns under the microcanonical (*NVE*) ensemble. The Tersoff potential 43 was used to describe the interatomic interactions among carbon atoms in the biochar film, and those among hydrogen and oxygen atoms in  $H_2O_2$  were defined by the consistent valence forcefield (CVFF). 44 The Lennard-Jones (LJ) potential was used to describe nonbonded interactions among the biochar and  $H_2O_2$  constituents.

Biochar films functionalized with different weight concentrations of ethylenediamine and nonadecanamide were also simulated. The Amber force field 45,46 was used to define interactions within and among ethylenediamine, and those of nonadecanamide were defined with CVFF. Four concentrations were examined: 1.2, 2.1, 5.6, and 10 wt %, corresponding to 5, 9, 25, and 48 ethylenediamine molecules and 1, 2, 5, and 9 nonadecanamide molecules, respectively. The simulations ran for 20 ns, tallying the number of  $\rm H_2O_2$  molecules having passed the film.

#### RESULTS AND DISCUSSION

Laboratory Results. Figure 1 shows the crossover modulus measured for unaged samples (0 h) and samples

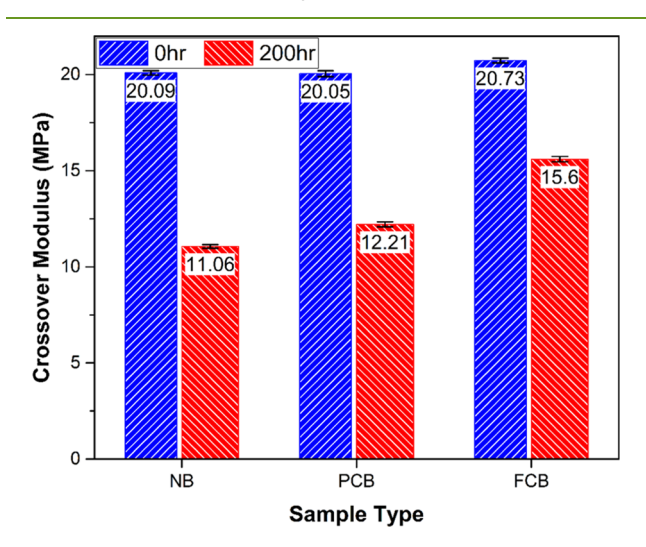


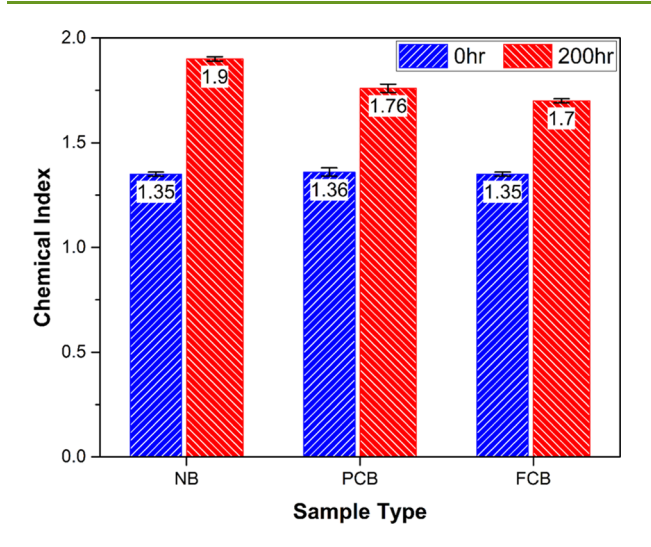
Figure 1. Crossover modulus for unaged (0 h) and UV-aged (200 h) samples.

Table 2. Rheological Aging Index for All Samples

	NB	PCB	FCB
rheological aging index (%)	45	39	25
improvement (%)		13	45

subjected to 200 h UV aging. All unaged samples showed almost the same crossover modulus values. This indicates that the biochar (PCB and FCB) did not have a significant influence on the stiffness of neat bitumen (NB). The impact of UV aging, however, proved to be significant. The crossover

(4)



**Figure 2.** Chemical index for all samples subjected to 0 and 200 h UV aging.

Table 3. Chemical Aging Index for All Samples

	NB	PCB	FCB
chemical aging index (%)	41	29	26
improvement (%)		28	35

modulus of the NB sample decreased by 45% from 20.09 to 11.06 MPa. The incorporation of PC into bitumen slightly enhanced the resistance of bitumen to UV aging: there was a 39% reduction in the crossover modulus for PCB. The FCB sample showed the least susceptibility to aging in terms of the crossover modulus (25%), demonstrating the efficacy of functionalized carbon in extending the life of pavements.

The more favorable performance of IFC in comparison with PC was also reflected in the rheological aging indexes of the samples. The results summarized in Table 2 show that IFC was more effective than PC in reducing the rheological aging index of neat bitumen (45% vs 13%).

A similar trend is observed in the chemical aging behavior of the samples (Figure 2). Although the chemical index of all samples increased after 200 h of UV aging, the neat bitumen showed the highest increase, followed by PCB and FCB. Comparison of the chemical aging indices calculated based on these data (Table 3) shows that both woody and algal biochars delayed the UV aging of neat bitumen, but the algal biochar was more effective.

MD Simulation Results. Figure 3 and the corresponding configurations (Figure 4) indicate that both ethylenediamine and nonadecanamide were effective in protecting the biochar film against the diffusion of  $H_2O_2$ , and they exhibited comparable efficacies at concentrations below about 5.6 wt %. However, while the efficacy of nonadecanamide peaked at this concentration, that of ethylenediamine continued to almost linearly increase over the entire concentration range studied. At a concentration of 10 wt %, for instance, ethylenediamine reduced the number of passed  $H_2O_2$ s by 34% (from 237 to 157), showing 12% more effectiveness than nonadecanamide (from 237 to 186).

#### CONCLUSIONS

We examined the merit of carbonaceous particles grafted by bioderived molecules (e.g., amines and amides) for scavenging free radicals. Our laboratory experiments and molecular dynamics simulations showed that the grafting of bioderived molecules can be tailored to maximize their scavenging capacity, as evidenced by the decreased diffusion of free radicals through biografted carbon particles. It was also shown that the application of functionalized carbon-modified binders remarkably delayed the aging of bituminous composites. While woody biochar (pristine biochar) improved the rheology-based and chemistry-based aging indexes of bituminous composites by 13 and 28%, respectively, the samples containing algal biochar (IFC) exhibited much higher improvement of 45 and 35% in the respective indexes. These observations were corroborated by our molecular dynamics simulations showing the increased barrier efficiency of biografted carbon against free radicals. The amine and amide functionals used in the simulations exhibited comparable efficacies at preventing the diffusion of H2O2 at low modifier concentrations. At high concentrations, however, the amine functionals proved to be

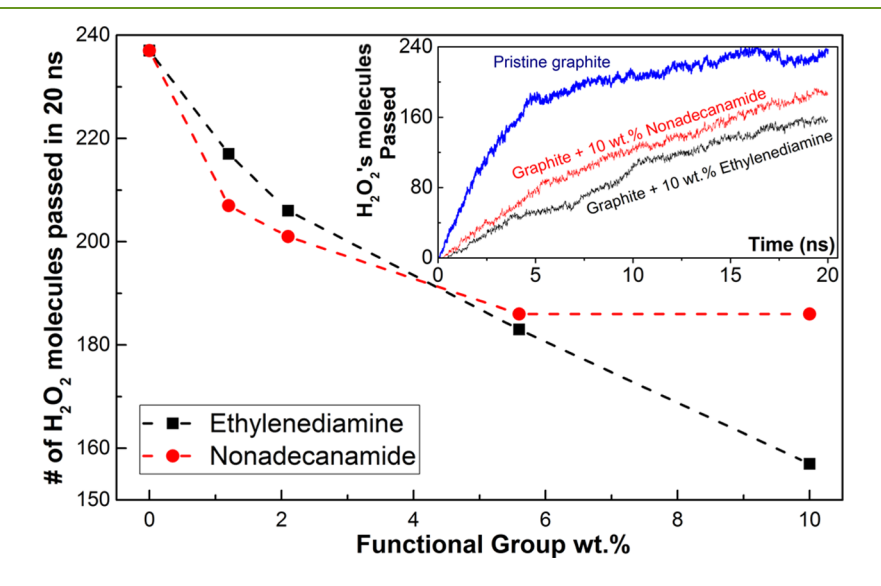


Figure 3. Efficacy of functional groups in reducing the diffusion of  $H_2O_2$  molecules into biochar; the inset shows the diffusion history of  $H_2O_2$  molecules into biochar in pristine, 10 wt % nonadecanamide, and 10 wt % ethylenediamine forms.

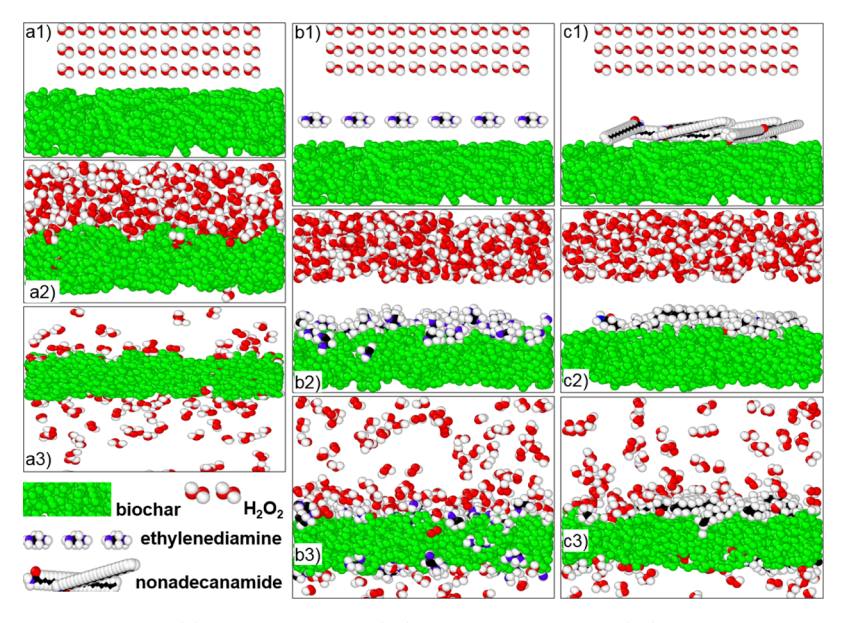


Figure 4. Diffusion of  $H_2O_2$  molecules into (a) pristine biochar: (a1) initial configuration, (a2) at t=80 ps corresponding to the first  $H_2O_2$  molecule reaching the other side of biochar, and (a3) at t=20 ns; (b) biochar functionalized with 10 wt % ethylenediamine: (b1) initial configuration, (b2) at equilibrium before allowing  $H_2O_2$  to interact with the rest of the model, and (b3) at t=20 ns; and (c) biochar functionalized with 10 wt % nonadecanamide: (c1) initial configuration, (c2) at equilibrium before allowing  $H_2O_2$  to interact with the rest of the model, and (c3) at t=20 ns. Note: T=300 K. The legend is shown at the bottom left.

more effective than amide functionals, indicating the scavenging capacity of biografted carbon can be further tuned using optimized grafting. The outcome of the study promotes the use of carbon derived from biomass to extend the service life of road infrastructure; this not only supports carbon sequestration and resource conservation but also promotes sustainable construction.

# AUTHOR INFORMATION

#### **Corresponding Author**

Elham H. Fini — School of Sustainable Engineering and the Built Environment, Ira A. Fulton Schools of Engineering, Arizona State University, Tempe, Arizona 85287-3005, United States; oorcid.org/0000-0002-3658-0006; Email: efini@asu.edu

#### **Authors**

Hamid Ghasemi – Department of Civil and Environmental Engineering, Howard University, Washington, District of Columbia 20059, United States

Hessam Yazdani — Department of Civil and Environmental Engineering, Howard University, Washington, District of Columbia 20059, United States; ⊚ orcid.org/0000-0003-4809-1362

Amirul Rajib — School of Sustainable Engineering and the Built Environment, Ira A. Fulton Schools of Engineering, Arizona State University, Tempe, Arizona 85287-3005, United States; orcid.org/0000-0002-9567-8986

Complete contact information is available at: https://pubs.acs.org/10.1021/acssuschemeng.1c07356

#### **Notes**

The authors declare no competing financial interest.

#### ACKNOWLEDGMENTS

This material was based upon work supported by the U.S. National Science Foundation under grants CBET 1935723 and

CMMI 2046332. The authors acknowledge supercomputing centers at the University of Oklahoma and Arizona State University for providing access to HPC resources. The authors appreciate the assistance of Dr. S. Shariati with Arizona State University with the design of the table of contents.

### **■** REFERENCES

- (1) Herrington, P. R.; Patrick, J. E.; Ball, G. F. A. Oxidation of Roading Asphalts. *Ind. Eng. Chem. Res.* **1994**, *33*, 2801–2809.
- (2) Hung, A.; Fini, E. H. Surface Morphology and Chemical Mapping of UV-Aged Thin Films of Bitumen. *ACS Sustainable Chem. Eng.* **2020**, *8*, 11764–11771.
- (3) Hung, A. M.; Fini, E. H. Absorption Spectroscopy to Determine the Extent and Mechanisms of Aging in Bitumen and Asphaltenes. *Fuel* **2019**, 242, 408–415.
- (4) Khare, P.; Machesky, J.; Soto, R.; He, M.; Presto, A. A.; Gentner, D. R. Asphalt-Related Emissions Are a Major Missing Nontraditional Source of Secondary Organic Aerosol Precursors. *Sci. Adv.* **2020**, *6*, No. eabb9785.
- (5) Mousavi, M.; Pahlavan, F.; Oldham, D.; Hosseinnezhad, S.; Fini, E. H. Multiscale Investigation of Oxidative Aging in Biomodified Asphalt Binder. *J. Phys. Chem. C* **2016**, *120*, 17224–17233.
- (6) Karnati, S. R.; Oldham, D.; Fini, E. H.; Zhang, L. Surface Functionalization of Silica Nanoparticles to Enhance Aging Resistance of Asphalt Binder. *Construct. Build. Mater.* **2019**, *211*, 1065–1072.
- (7) Mousavi, M.; Fini, E. Silanization Mechanism of Silica Nanoparticles in Bitumen Using 3-Aminopropyl Triethoxysilane (APTES) and 3-Glycidyloxypropyl Trimethoxysilane (GPTMS). ACS Sustainable Chem. Eng. 2020, 8, 3231–3240.
- (8) Apeagyei, A. K. Laboratory Evaluation of Antioxidants for Asphalt Binders. *Construct. Build. Mater.* **2011**, *25*, 47–53.
- (9) Cong, P.; Xu, P.; Chen, S. Effects of Carbon Black on the Anti Aging, Rheological and Conductive Properties of SBS/Asphalt/ Carbon Black Composites. *Construct. Build. Mater.* **2014**, *52*, 306–313
- (10) Wu, S.; Han, J.; Pang, L.; Yu, M.; Wang, T. Rheological Properties for Aged Bitumen Containing Ultraviolate Light Resistant Materials. *Construct. Build. Mater.* **2012**, *33*, 133–138.
- (11) Xu, S.; Yu, J.; Zhang, C.; Sun, Y. Effect of Ultraviolet Aging on Rheological Properties of Organic Intercalated Layered Double

- Hydroxides Modified Asphalt. *Construct. Build. Mater.* **2015**, 75, 421–428.
- (12) Zhang, C.; Yu, J.; Xu, S.; Xue, L.; Cao, Z. Influence of UV Aging on the Rheological Properties of Bitumen Modified with Surface Organic Layered Double Hydroxides. *Construct. Build. Mater.* **2016**, 123, 574–580.
- (13) Cao, Z.; Chen, M.; He, B.; Han, X.; Yu, J.; Xue, L. Investigation of Ultraviolet Aging Resistance of Bitumen Modified by Layered Double Hydroxides with Different Particle Sizes. *Construct. Build. Mater.* **2019**, *196*, 166–174.
- (14) Zhu, B.; Chen, G.; Cao, X.; Wei, D. Molecular Characterization of CO2 Sequestration and Assimilation in Microalgae and Its Biotechnological Applications. *Bioresour. Technol.* **2017**, 244, 1207–1215.
- (15) Markou, G.; Nerantzis, E. Microalgae for High-Value Compounds and Biofuels Production: A Review with Focus on Cultivation under Stress Conditions. *Biotechnol. Adv.* **2013**, *31*, 1532—1542.
- (16) Michael, S.; Sundaramahalingam, M.; Shivamthi, C. S.; Shyam Kumar, R.; Perumal, V.; Karthikumar, S.; Kanimozhi, J. Insights about Sustainable Biodiesel Production from Microalgae Biomass: A Review. *Int. J. Energy Res.* **2021**, *45*, 17028–17056.
- (17) Mousavi, M.; Martis, V.; Fini, E. H. Inherently Functionalized Carbon from Algae to Adsorb Precursors of Secondary Organic Aerosols in Noncombustion Sources. *ACS Sustainable Chem. Eng.* **2021**, *9*, 14375–14384.
- (18) Shao, J.; Zhang, J.; Zhang, X.; Feng, Y.; Zhang, H.; Zhang, S.; Chen, H. Enhance SO2 Adsorption Performance of Biochar Modified by CO2 Activation and Amine Impregnation. *Fuel* **2018**, 224, 138–146.
- (19) Chen, W.; Chen, Y.; Yang, H.; Li, K.; Chen, X.; Chen, H. Investigation on Biomass Nitrogen-Enriched Pyrolysis: Influence of Temperature. *Bioresour. Technol.* **2018**, 249, 247–253.
- (20) Reddy Karnati, S.; Høgsaa, B.; Zhang, L.; Fini, E. H. Developing Carbon Nanoparticles with Tunable Morphology and Surface Chemistry for Use in Construction. *Construct. Build. Mater.* **2020**, 262, 120780.
- (21) Fini, E.; Rajib, A. I.; Oldham, D.; Samieadel, A.; Hosseinnezhad, S. Role of Chemical Composition of Recycling Agents in Their Interactions with Oxidized Asphaltene Molecules. *J. Mater. Civ. Eng.* **2020**, 32, 04020268.
- (22) Rajib, A.; Fini, E. H. Inherently Functionalized Carbon from Lipid and Protein-Rich Biomass to Reduce Ultraviolet-Induced Damages in Bituminous Materials. *ACS Omega* **2020**, *5*, 25273–25280.
- (23) Zhang, X.; Xiang, W.; Wang, B.; Fang, J.; Zou, W.; He, F.; Li, Y.; Tsang, D. C. W.; Ok, Y. S.; Gao, B. Adsorption of Acetone and Cyclohexane onto CO2 Activated Hydrochars. *Chemosphere* **2020**, 245, 125664.
- (24) Pahlavan, F.; Samieadel, A.; Deng, S.; Fini, E. Exploiting Synergistic Effects of Intermolecular Interactions To Synthesize Hybrid Rejuvenators To Revitalize Aged Asphalt. *ACS Sustainable Chem. Eng.* **2019**, *7*, 15514–15525.
- (25) Pahlavan, F.; Rajib, A.; Deng, S.; Lammers, P.; Fini, E. H. Investigation of Balanced Feedstocks of Lipids and Proteins To Synthesize Highly Effective Rejuvenators for Oxidized Asphalt. ACS Sustainable Chem. Eng. 2020, 8, 7656.
- (26) Fini, E. H.; Samieadel, A.; Rajib, A. Moisture Damage and Its Relation to Surface Adsorption/Desorption of Rejuvenators. *Ind. Eng. Chem. Res.* **2020**, *59*, 13414–13419.
- (27) Dandamudi, K. P. R.; Murdock, T.; Lammers, P. J.; Deng, S.; Fini, E. H. Production of Functionalized Carbon from Synergistic Hydrothermal Liquefaction of Microalgae and Swine Manure. *Resour. Conserv. Recycl.* **2021**, *170*, 105564.
- (28) Rajib, A.; Saadeh, S.; Katawal, P.; Mobasher, B.; Fini, E. H. Enhancing Biomass Value Chain by Utilizing Biochar as A Free Radical Scavenger to Delay Ultraviolet Aging of Bituminous Composites Used in Outdoor Construction. *Resour. Conserv. Recycl.* **2021**, *168*, 105302.

- (29) Yu, J.-Y.; Feng, P.-C.; Zhang, H.-L.; Wu, S.-P. Effect of Organo-Montmorillonite on Aging Properties of Asphalt. *Construct. Build. Mater.* **2009**, 23, 2636–2640.
- (30) ASTM D7175-05. Standard Test Method for Determining the Rheological Properties of Asphalt Binder Using a Dynamic Shear Rheometer. In *Annual Book of ASTM Standards*; ASTM International: West Conshohocken, PA, 2017; Vol. 04.03.
- (31) Samieadel, A.; Oldham, D.; Fini, E. H. Investigating Molecular Conformation and Packing of Oxidized Asphaltene Molecules in Presence of Paraffin Wax. *Fuel* **2018**, 220, 503–512.
- (32) Rajib, A. I.; Pahlavan, F.; Fini, E. H. Investigating Molecular-Level Factors That Affect the Durability of Restored Aged Asphalt Binder. *J. Clean. Prod.* **2020**, *270*, 122501.
- (33) Rajib, A. I.; Samieadel, A.; Zalghout, A.; Kaloush, K. E.; Sharma, B. K.; Fini, E. H. Do All Rejuvenators Improve Asphalt Performance? *Road Mater. Pavement Des.* **2020**, *0*, 1–19.
- (34) Oldham, D. J.; Obando, C. J.; Mousavi, M.; Kaloush, K. E.; Fini, E. H. Introducing the Critical Aging Point (CAP) of Asphalt Based on Its Restoration Capacity. *Construct. Build. Mater.* **2021**, 278, 122379.
- (35) Simoneit, B. R. T.; Rushdi, A. I.; bin Abas, M. R.; Didyk, B. M. Alkyl Amides and Nitriles as Novel Tracers for Biomass Burning. *Environ. Sci. Technol.* **2003**, *37*, 16–21.
- (36) Ross, A. B.; Biller, P.; Kubacki, M. L.; Li, H.; Lea-Langton, A.; Jones, J. M. Hydrothermal Processing of Microalgae Using Alkali and Organic Acids. *Fuel* **2010**, *89*, 2234–2243.
- (37) Chen, W.; Yang, H.; Chen, Y.; Xia, M.; Chen, X.; Chen, H. Transformation of Nitrogen and Evolution of N-Containing Species during Algae Pyrolysis. *Environ. Sci. Technol.* **2017**, *51*, 6570–6579.
- (38) Leng, L.; Xu, S.; Liu, R.; Yu, T.; Zhuo, X.; Leng, S.; Xiong, Q.; Huang, H. Nitrogen Containing Functional Groups of Biochar: An Overview. *Bioresour. Technol.* **2020**, 298, 122286.
- (39) Voskian, S.; Brown, P.; Halliday, C.; Rajczykowski, K.; Hatton, T. A. Amine-Based Ionic Liquid for CO2 Capture and Electrochemical or Thermal Regeneration. *ACS Sustainable Chem. Eng.* **2020**, *8*, 8356–8361.
- (40) Kumar, D. R.; Rosu, C.; Sujan, A. R.; Sakwa-Novak, M. A.; Ping, E. W.; Jones, C. W. Alkyl-Aryl Amine-Rich Molecules for CO2 Removal via Direct Air Capture. *ACS Sustainable Chem. Eng.* **2020**, *8*, 10971–10982.
- (41) Mattsson, T. R.; Lane, J. M. D.; Cochrane, K. R.; Desjarlais, M. P.; Thompson, A. P.; Pierce, F.; Grest, G. S. First-Principles and Classical Molecular Dynamics Simulation of Shocked Polymers. *Phys. Rev. B: Condens. Matter Mater. Phys.* **2010**, *81*, 054103.
- (42) van Duin, A. C. T.; Dasgupta, S.; Lorant, F.; Goddard, W. A. ReaxFF: A Reactive Force Field for Hydrocarbons. *Phys. Chem. A* **2001**, *105*, 9396–9409.
- (43) Tersoff, J. Modeling Solid-State Chemistry: Interatomic Potentials for Multicomponent Systems. *Phys. Rev. B: Condens. Matter Mater. Phys.* **1989**, *39*, 5566–5568.
- (44) Hagler, A. T.; Lifson, S.; Dauber, P. Consistent Force Field Studies of Intermolecular Forces in Hydrogen-Bonded Crystals. 2. A Benchmark for the Objective Comparison of Alternative Force Fields. *J. Am. Chem. Soc.* **1979**, *101*, 5122–5130.
- (45) Balabaev, N. K.; Belashchenko, D. K.; Rodnikova, M. N.; Kraevskii, S. V.; Solonina, I. A. Modeling the Structure of Liquid Monoethanolamine by Molecular Dynamics. *Russ. J. Phys. Chem. A* **2015**, *89*, 398–405.
- (46) Balabaev, N. K.; Kraevskii, S. V.; Rodnikova, M. N.; Solonina, I. A. Molecular-Dynamic Study of Liquid Ethylenediamine. *Russ. J. Phys. Chem. A* **2016**, *90*, 1986–1992.